46th Annual Review of Progress
in Quantitative Nondestructive Evaluation
QNDE2019
July 14-18, 2019, Portland, OR, USA

QNDE2019-1234

CONFORMAL COAXIAL HELICAL ANTENNA FOR DISTRIBUTED SENSING APPLICATIONS AT WELLBORES

Roman Shugayev[1], Jagannath Devkota, Paul Ohodnicki
NETL
Pittsburgh, PA

ABSTRACT

Microstrip antennas on nonplanar substrates can exhibit nontrivial radiation behavior. In this work we demonstrate efficient conversion of radiation from microstrip antennas helically wound on the coaxial cable to external coaxial mode for distributed sensing and power delivery in wellbore environments. The same approach may also have broad applications in other energy, civil, and industrial infrastructure applications where embedded wireless sensor networks are deployed.

Keywords: microstrip antennas, array antennas, wireless sensing

1. INTRODUCTION

In the fields of industrial and wireless sensing, the communication channel often determines the characteristics and performance of the overall sensing network. For wellbore monitoring applications, telemetry challenges are particularly acute due to (1) harsh environmental conditions (elevated temperature and pressure, chemically corrosive, etc.) which restrict the application of complex electronics and instrumentation; and (2) inherent absorption of electromagnetic radiation within the subsurface environment which also severely limits the potential for free space wireless power and signal delivery over significant distances. High absorption in the downhole is directly linked to high content of water, i.e. in typical oil-bearing deposit decay length is 1.06 m for 36% water saturated shale and 8.5 cm for concrete @ 1 GHz [1,2]. Nevertheless, distributed wireless sensors throughout the subsurface environment would provide unprecedented visibility from the perspective of monitoring and minimizing environmental impacts associated with the wellbore as well as ensuring safe and productive operation of oil and gas recovery processes, enhanced geothermal systems and carbon storage sites.

One example potential deployment scheme for wireless and passive sensors is to position them throughout the wellbore cement and on the exterior of a wellbore casing (Figure 1). However, the challenges of wireless telemetry greatly complicate the system design and have historically precluded deployment. One approach to microwave telemetry being investigated for such demanding applications is the implementation of a dedicated guiding channel for long haul telemetry and with distributed antennas for short distance wireless links with deployed sensors. This approach retains much of the advantages inherent with truly free-space wireless sensor networks such as mitigating the need for active electronics in the high temperature and pressure subsurface environment.

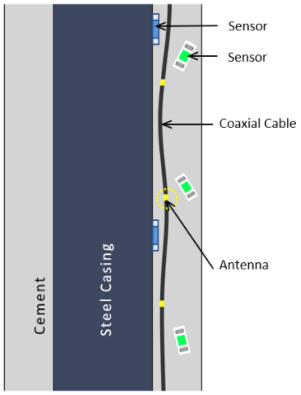

FIGURE 1: WELBORE SENSING METHODOLOGY

A promising avenue to fulfill requirements for power transfer and ease of installation in this method is to use conformal antennas integrated periodically on a coaxial cable-based interrogator that could be designed to convert the radiation into propagating external mode of the coaxial cable. This approach would keep radiated power confined to cement region around the casing where coaxial cable and sensors are placed instead of being freely radiated and lost which would be the case when using conventional free space antennas. An added advantage of this approach is that it would permit utilization of antennas as local permittivity probes capable of detecting

[1] Contact author: roman.shugayev@netl.doe.gov

environmental changes in the wellbore, such as increase in water content in cement and surrounding formations.

In this work we present an early example design based upon conformal coaxial helical antennas. The helical antenna probe is comprised of helical microstrip antenna, antenna feed and coaxial cable serving as a channel for long haul power and signal delivery as well as external mode guiding (Fig.2).

2. SYSTEM DESIGN

Coaxial cable waveguiding structure in our design supports internal as well as external TEM propagating modes. We can view end-fire emission of helical antenna on top of the cylinder as a coupling problem between the helical current source on the surface of coaxial cable and the external TEM mode of the coax. From this point of view to induce efficient coupling the phase relation between the currents in neighboring turns has to correspond to the phase relation of the TEM wave traveling with a velocity $v \approx v_0$.

Allowed external TEM mode propagation is bidirectional which permits us to consider both forward and reverse propagating waves for coupling. Since the microstrip mode traveling around the cylinder is inherently slower than the TEM wave traveling in the same direction we choose to induce coupling to the backward propagating wave.

The phase matching condition becomes

$$\frac{n \cdot S}{\lambda_0} = 1 - \frac{n \cdot L_0 \cdot \sqrt{e_{eff}}}{\lambda_0} \qquad (1)$$

Where $L_0 = \sqrt{C^2 + S^2}$, C and S are circumference of the single loop and spacing between helical turns, n is the number of turns ($n = 1$ for design purposes). Left hand side of this equation corresponds to fractional phase shift of external TEM mode and the right-hand side is a phase shift of the microstrip current in the helical antenna.

Design frequency was set to $f_0 = 3.35$ GHz with corresponding $\lambda_0 = 8.95\ cm$. The frequency readily applies to several existing microwave sensing technologies such as wireless solid-state sensors and surface acoustic wave sensors.

Geometrical parameters were set to $C = 2\pi r = 1.53 \cdot \lambda_0$, $S = 0.1508 \cdot \lambda_0$. In our design we assumed the effective permittivity, e_{eff} of the microstrip to be that of planar microstrip with $W/\mathrm{H} > 1$ (in our case W= 0.8 mm and H =0.5 mm). Using formula (1) we determine $e_{eff} = 1.607$ and by solving implicit equation [3]

$$e_{eff} = \frac{e_{sub}+1}{2} + \frac{e_{sub}-1}{2}\left(1 + 12\frac{W}{H}\right)^{-1/2} \qquad (2)$$

we obtain substrate permittivity $e_{sub} = 1.907$. These parameter values produced effective phase between currents in neighboring turns of $\varphi = 53°$.

The number of turns for the antenna was set to N=7. This corresponds to total length of the helix is $L = N \cdot S = 1.05 \cdot \lambda_0$ and approximately equals to one period, which ensures even excitation of all temporal phases.

For the purpose of this study both coax and microstrip impendences were kept at Z0=79.6 Ohms which was determined by the microstrip velocity required for traveling wave coupling to TEM mode. The excitation port 1 and the through port 2 were both matched to Z0. For this work we analyze a truncated coaxial cable with a length of L=0.28 m closely representing behavior of semi-infinite cable.

For our modeling we used commercial finite element method implemented in COMSOL to estimate antenna local fields, far field parameters and corresponding S-parameters.

3. RESULTS AND DISCUSSION

We were able to obtain a good matching of the antenna emission to the external mode of the coaxial cable. Resonant frequency of the coupling was determined to be $f_0 = 3.38$ GHz which exhibit two end-fire radiation peaks without any nulls in axial (x) direction (Fig. 3(b)). Electric field distribution corresponding to propagating external mode confined to coaxial cable can also be clearly observed (Fig. 2(b)).

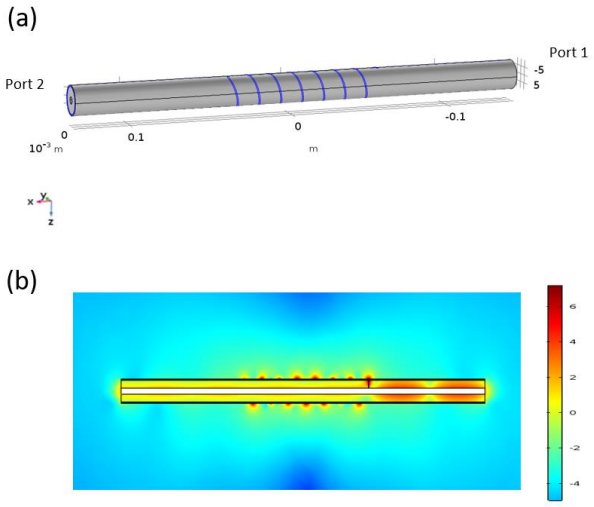

FIGURE 2: ANTENNA GEOMETRY (A) AND LOGARITHM OF ELECTRIC FIELD MAGNITUDE AT F=3.38 GHZ (XZ PLANE) (B)

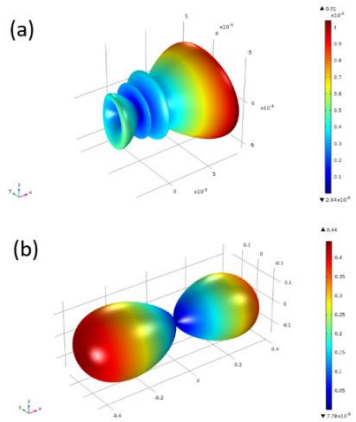

FIGURE 3: FAR FIELD EMITTED POWER. (A) F=2.13 GHZ (B) F=3.38 GHZ

As frequency is shifted from the resonant frequency (Fig. 3,4) the null at the helical axis gradually appears. Additionally, sidelobes progressively grow in number at the lower frequencies (Fig.3 (a)) corresponding to the minima of the S21 parameters, contrary to the normal end-fire array behavior where number of sidelobes decreases with increasing wavelength [4,5].

The emission is double-sided due to the back reflected wave at the discontinuity of the helix. From analysis of 2D emission plots we also observed that the coupling is more efficient (by 15%) in the negative X direction.

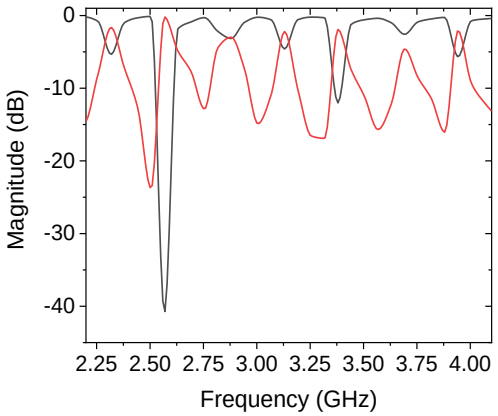

FIGURE 4: S-PARAMETERS. S11 (RED), S21 (BLACK)

The S11/S21 magnitude exhibits oscillations in the frequency domain corresponding to the phase matching condition at multiple turns in Equation 1. While the side peaks at f=3.63 and f=3.94 GHz have certain energy coupled to the axial mode overall their emission is less efficient than for competing off-axis directions. The peak at f=3.13 GHz has no nulls in axial direction however contains a minor sidelobe. The off-center peaks may be used for a reduced power fractional emission required for multiple sensors coupled to the same coaxial cable.

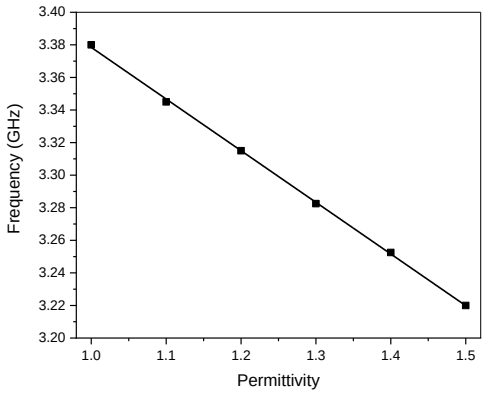

FIGURE 5 FREQUENCY OF THE RESONANT DEEP OF S21 VS PERMITTIIVTY OF THE MEIDUM

Previously microstrip antennas have been considered for moisture and salinity sensing using simple patch geometries [6,7]. To analyze sensitivity of our design to environmental parameters we have varied external permittivity of coaxial cable while monitoring resonant dip in S21 at f=3.38 GHz (Fig. 5). The probe exhibits linear sensitivity to the external medium permittivity in the range $(1-1.5)$ with a slope of 0.31 GHz/piu (permittivity index unit). In the case $e_{medium} \neq 1$ effective phase shift of the TEM mode in Equation 1 is reduced by $\sqrt{e_{medium}}$. The microstrip e_{eff} in this case can be described by linear relation $e_{eff} = k_1 \cdot e_{medium} + k_2 \cdot e_{eff}$ [8] with contributions due to flux confined in the microstrip substrate and fringing through external medium. For the analyzed geometry coefficients were determined to be $k_1 = 0.164$ and $k_2 = 0.836$.

4. CONCLUSION

Demonstrated efficient coupling of proposed antenna design to the TEM mode of coaxial cable should make it an attractive option for distributed power, signal delivery and remote sensing.

Resonant character of the observed emission would permit the usage of such antennas for distributed applications and direct environmental parameter sensing enabling selective frequency access of individual sensors.

REFERENCES

[1] Sweeney, Jerry J., Jeffery J. Roberts, and Philip E. Harben. "Study of dielectric properties of dry and saturated green river oil shale." *Energy & Fuels* 21.5 ,2007

[2] Baker-Jarvis, James R., Michael D. Janezic, Billy F. Riddle, Robert T. Johnk, Christopher L. Holloway, Richard G. Geyer, and Chriss A. Grosvenor. Measuring the Permittivity and Permeability of Lossy Materials: Solids, Liquids, Metals, and negative-Index Materials. *No. Technical Note (NIST TN)-1536*, 2005

[3] Bahl, Inder J. "A designer's guide to microstrip line." *Microwaves* , 1977

[4] Constantine, A. Balanis. "Antenna theory: analysis and design." MICROSTRIP ANTENNAS, third edition, *John wiley & sons*, 2005

[5] J.D. Kraus, "Atennas", *McGraw-Hill*, 1988

[6] Lee, Kibae, et al. "Microstrip patch sensor for salinity determination." *Sensors* 17.12, 2017

[7] Jain, Sweety, et al. "Microstrip Moisture Sensor Based on Microstrip Patch Antenna." *Progress In Electromagnetics Research* 76, 2018

[8] Darwish, Ali, et al. "Properties of the embedded transmission line (ETL)-an offset stripline with two dielectrics." *IEEE Microwave and Guided Wave Letters* , 1999